

Qri7/OSGEPL, the mitochondrial version of the universal Kae1/YgjD protein, is essential for mitochondrial genome maintenance

Jacques Oberto¹, Norman Breuil¹, Arnaud Hecker¹, Francesca Farina¹,
Céline Brochier-Armanet^{2,3}, Emmanuel Culetto^{1,*} and Patrick Forterre^{1,4,*}

¹Université Paris-Sud 11, CNRS, UMR8621, Institut de Génétique et Microbiologie, 91405 Orsay, ²Institut de Microbiologie de la Méditerranée (IFR88), Laboratoire de Chimie Bactérienne, UPR9043-CNRS, 13402 Marseille Cedex 20, ³Université de Provence – Aix-Marseille I, 13331 Marseille Cedex 3 and ⁴Institut Pasteur, Unité Biologie Moléculaire du Gène chez les Extrêmophiles, 25 rue du Dr Roux, 75724 Paris Cedex 15, France

Received February 26, 2009; Revised and Accepted June 15, 2009

ABSTRACT

Yeast Qri7 and human OSGEPL are members of the orthologous Kae1(OSGEP)/YgjD protein family, the last class of universally conserved proteins without assigned function. Phylogenetic analyses indicate that the eukaryotic Qri7(OSGEPL) proteins originated from bacterial YgjD proteins. We have recently shown that the archaeal Kae1 protein is a DNA-binding protein that exhibits apurinic endonuclease activity *in vitro*. We show here that the Qri7/OSGEPL proteins localize in mitochondria and are involved in mitochondrial genome maintenance in two model eukaryotic organisms, *Saccharomyces cerevisiae* and *Caenorhabditis elegans*. Furthermore, *S. cerevisiae* Qri7 complements the loss of the bacterial YgjD protein in *Escherichia coli*, suggesting that Qri7/OSGEPL and YgjD proteins have retained similar functions in modern organisms. We suggest to name members of the Kae1(OSGEP)/YgjD family UGMP, for Universal Genome Maintenance Proteins.

INTRODUCTION

The *KAE1/osgep/ygjD* gene family constitutes the only class of the universally conserved gene set that still remains without an assigned function and merits therefore a particular attention. The genome of all completely sequenced organisms harbors at least one member of the *KAE1/osgep/ygjD* gene family with only two exceptions, the highly reduced genomes of *Carsonella ruddii* and *Sulcia muelleri* (1–3). Despite their universal distribution,

the precise function of these proteins, which are known under different names (YgjD/Gcp and YeaZ in Bacteria, Kae1 in Archaea, Kae1p and Qri7p in yeast, OSGEP and OSGEPL in human), remains largely unknown. In *Manheimia haemolytica* (formerly *Pasteurella haemolytica*), the Gcp protein was reported to encode an *O*-sialoglycoprotein endopeptidase (4,5), hence the name of the yeast and human proteins (Kae1 for kinase-associated endopeptidase, and OSGEP for *O*-sialoglycoprotein endopeptidase, respectively). However, purified bacterial and archaeal homologs of these proteins, the *Escherichia coli* YeaZ and the *Pyrococcus abyssi* Kae1 proteins, respectively, do not show such activity *in vitro* (2,6).

The universal genomic distribution, lack of determined function and misannotation of this protein family warrant the priority and importance of its study (7). It has been reported two years ago that the yeast Kae1 protein is part of the chromatin associated multi-protein complex KEOPS/EKC that is required for telomere maintenance and efficient gene transcription of essential genes (8–10). It was proposed that Kae1 controls the activity of this complex via its proteolytic activity. However, we found later on that the *P. abyssi* Kae1 protein is an atypical DNA-binding protein that exhibits an unusual apurinic endonuclease activity *in vitro* (2), suggesting instead that Kae1 plays a direct role in genome stability maintenance by anchoring the KEOPS/EKC complex to chromatin.

Interestingly, most eukaryotes harbor two distantly related homologs that branch in different parts of the phylogenetic tree of the whole family (2). One copy forms a monophyletic group that includes the yeast Kae1 protein identified in the Keops/EKC complex. This group branches with archaeal sequences suggesting that it was inherited from the common ancestor of Archaea

*To whom correspondence should be addressed. Tel: +33 1 69 15 74 89; Fax: +33 1 69 15 78 08; Email: patrick.forterre@igmors.u-psud.fr
Correspondence may also be addressed to Emmanuel Culetto. Tel: +33 1 69 82 43 81; Fax: +33 1 69 82 43 86; Email: emmanuel.culetto@u-psud.fr

The authors wish it to be known that, in their opinion, the first two authors should be regarded as joint First Authors.

and Eukarya. In contrast, the second copy found in eukaryotes (dubbed Qri7 in the yeast *Saccharomyces cerevisiae* and OSGEPL in human) emerges from within bacterial YgjD proteins, suggesting a mitochondrial origin (2). These hypotheses are in agreement with data obtained in *S. cerevisiae* showing that Kae1p is cytoplasmic/nuclear whereas Qri7p is predicted to be mitochondrial, according to the yeast GFP Fusion Localization Database (11). Moreover, a *qri7*Δ mutant exhibits growth defect on non-fermentable carbon sources, such as glycerol or lactate, suggesting that Qri7 is essential for mitochondrial physiology (12). Similarly, the *E. coli ygjD* mutation is lethal (13,14). These observations, together with our recent finding that the archaeal Kae1 protein is probably involved in DNA metabolism, suggested that Qri7/OSGEPL proteins could be involved in mitochondrial genome maintenance. To test this hypothesis, we investigated the properties of Qri7/OSGEPL proteins in two eukaryotic model organisms, *S. cerevisiae* and *Caenorhabditis elegans*.

MATERIALS AND METHODS

Strains, media and growth conditions

The construction of the conditional *ygdD* *E. coli* strain (JO93) was carried out as described by Datsenko and Wanner (15). Briefly, *E. coli* strain BW25141 carrying the Red helper plasmid pKD46 and (pBADN-KmR)::*ygdD* was electroporated with a PCR product obtained by amplifying a CmR determinant with oligonucleotides complementary to sequences located upstream and downstream of the *ygdD* open reading frame. Colonies were selected at 37°C on complete medium containing kanamycin, chloramphenicol and arabinose. These colonies were then screened for ampicillin sensitivity at 42°C, to test for the loss of the Red helper plasmid. In order to yield JO93, the *ΔygdD::cmR* disruption was subsequently transferred to a different genetic background by P1 transduction (16). The recipient strain was C600 (Pasteur Institute) containing (pBADN-KmR)::*ygdD*. *E. coli* strains were grown at 37°C in LB (Luria Bertani) broth or LB-agar supplemented with the appropriate antibiotics. *S. cerevisiae* strains from the Euroscarf collection: Y00000 (BY4741, MATa, his3Δ1, leu2Δ0, met15Δ0, ura3Δ0), equivalent to SC288c and Y03801 (BY4741, MATa, his3Δ1, leu2Δ0, met15Δ0, ura3Δ0, YDL104c::kanMX4) were obtained from Bernard Dujon. *S. cerevisiae* strains were grown at 30°C on YPD, YPD-agar, YPG-agar (17). *Caenorhabditis elegans* strains, namely the wild-type N2, *unc-119(ed3)III*, *eri-1(mg366)IV* and *cep-1(lg12501)I* strains were obtained from the CGC; the *pmyo-3::mitochondrial signal sequence::GFP* strain was provided by Dr Marta Atal Sanz. The *osgl-1* gene was inactivated using the double-stranded RNA interference using the feeding method (18). The *C. elegans* double-mutant *eri-1(mg366)IV;cep-1(lg12501)I* was constructed as follows. We crossed *cep-1(lg12501)* male with *eri-1(mg366)* hermaphrodite using standard genetic protocol. The F1 cross progeny worms have been individualized on NGM plates to lay eggs for 24h. Selected F1 were

subsequently genotyped by PCR for the presence of both insertion in the *eri-1* gene, using primers gk138if, gk138ir, gk138ef and gk138er, and deletion in the *cep-1* gene using primers *eri-1f* and *eri-1r*. Ten F2 worms from F1 showing both polymorphisms were individualized to establish lines. The founder worm and 10 F3 were subsequently genotyped by PCR to select homozygous *eri-1(mg366)IV;cep-1(lg12501)I* lines that only segregate worms harboring both PCR polymorphisms.

Plasmids and cloning methodology

Plasmid (pBADN-KmR)::*ygdD* was constructed as follows: the parental plasmid pBADN-KmR derived from pBAD24 (19); its unique NdeI restriction site was eliminated by restriction with this enzyme, by Klenow DNA polymerase treatment and subsequent re-ligation. The unique NcoI site was converted to NdeI by site-directed mutagenesis using the Stratagene Quickchange protocol. The *apR* determinant was inactivated and replaced by cloning, into its unique ScaI site, a HincII fragment carrying the *kmR* gene from pUC4K (Pharmacia). The *E. coli ygdD* open reading frame was amplified by PCR using oligonucleotide primers Y1 and Y2 (Supplementary Table S3) from a genomic DNA template prepared as indicated below and cloned between the NdeI and BamHI sites downstream the arabinose operon promoter of pBADN-KmR. Vector pZE-JO was constructed by assembling modules originating from plasmids pZE12-luc, pZE21-MSC1 and pZA31-luc (20). An AatII-SacI fragment carrying the ampicillin resistance determinant, an AatII-AvrII fragment of carrying the P_L-tet0-1 promoter and the cloning polylinker and a SacI-AvrII fragment carrying the p15A origin of replication were ligated to generate pZE-JO. The open reading frames corresponding to the genes from the bacterial and yeast KAE1/OSGEG family were amplified by polymerase chain reaction using *Pfu* polymerase (Promega and Fermentas) using the appropriate genomic DNA templates, the oligonucleotides shown in Supplementary Table S3, and conditions recommended by the suppliers. PCR fragments were gel purified, digested with the appropriate restriction enzymes and cloned in plasmid pZE-JO. *E. coli* DNA was purified according to Silhavy *et al.* (16) and *S. cerevisiae* DNA was purified with the Wizard[®] SV Genomic DNA kit (Promega). High fidelity PCR system (Invitrogen) was used to amplify a fragment containing 1.5-kb upstream of *osgl-1* start codon and the genomic-coding sequence up to the last coding codon. The primers used to amplify the *osgl-1* genomic fragment were: *osgl-1GFPf* and *osgl-1GFPr* (Supplementary Table S3). The PCR product was digested with SalI and cloned in the SalI site of the pPD9575 vector (Fire A., pers. comm.) to produce pPD-*osgl-1::gfp*. The pPD-*osgl-1::gfp* vector was used for transgenic transformation using a BioRad Biolistic PDS-1000/HE (BioRad Laboratories, Hercules, CA, USA49) as described by Praitis *et al.* (21). The plasmid containing the *C. elegans osgl-1* gene fused at the C-terminus with GFP and under the control of *pie-1*-regulatory sequences was constructed in three steps using the Gateway cloning technology (22). In the first

step, the *osgl-1::gfp* fusion was amplified from pPD-*osgl-1::gfp* with primers C01att76f and AttGFPr containing 18 bases from the *osgl-1* genomic and *gfp* sequences, plus the attB1 or the attB2 sequences (Table S3). The attB-PCR product was then cloned into the entry vector named pDONR201 by a BP recombination reaction (Invitrogen) to produce pENTR-*osgl-1::gfp*. In the third step, the *osgl-1::gfp* fragment flanked by the two attL sequences in pENTR-*osgl-1::gfp* was transferred to the destination vector pID2.02 (23) by LR reaction to produce the pID-*osgl-1::gfp*. The destination vector contains *pie-1* regulatory elements, as well as *unc-119(+)*. The vector pID-*osgl-1::gfp* was introduced into *unc-119(ed3)* worms by biolistic bombardment to create integrated lines, as described above.

In silico analyses

The homologs of the KAE1/QRI7/YGJD family from all complete genomes available at the NCBI in June 2008 were retrieved using the BLASTp program (24). A multiple alignment of the retrieved homologs was performed using MUSCLE (25). The resulting alignment was then visually inspected and manually refined using ED programs from the MUST package (26). Regions where the homology between sites was doubtful were removed from the phylogenetic analysis. A subset of sequences representative of the diversity of the whole family (but excluding the bacterial very divergent YeaZ sequences) was selected and used for phylogenetic analysis. The resulting tree was constructed with Bayesian methods using the program MrBAYES 3.1.2 with a mixed substitution model and a gamma law (four rate categories) and a proportion of invariant sites to take among-site rate variation into account (27). The Markov chain Monte Carlo search was run with four chains for 1 000 000 generations, with trees being sampled every 100 generations (the first 2500 trees were discarded as 'burnin').

Sequence analysis

The sequence of Qri7p was used to perform a BLASTp search of the *C. elegans* genome at http://www.sanger.ac.uk/Projects/C_elegans/blast_server.shtml. We used default parameters as set on the site at the Sanger Center with the filters in place. The C01G10.10 gene was identified as the only matching candidate. The ClustalX tool (<http://www.ch.embnet.org/software/ClustalW.html>) was used to perform multiple sequence alignments. BoxShade (http://www.ch.embnet.org/software/BOX_form.html) was used for the graphical representation of sequence alignments and similarity analysis. Prediction of the mitochondrial localization was carried out by Mitoprot (<http://ihg.gsf.de/ihg/mitoprot.html>). The BAGET web server (<http://archaea.u-psud.fr/bin/baget.dll>) provided assistance for the identification the open reading frames and the design of the oligonucleotides for bacterial gene cloning (28).

PCR amplification of *S. cerevisiae* total DNA

Total DNA from strains SC288C (WT) and Y03801 (*qri7Δ*) was extracted as described (29) and subjected to

30 cycles of PCR amplification reactions with GoTaq DNA polymerase using three pairs of oligonucleotides: K1-pZE and K2-pZE, MT1-MT2 and MT3-MT4 (Supplementary Table S3).

RNA-mediated interference (RNAi)

Caenorhabditis elegans genes were inactivated using the double-stranded RNA interference using the feeding method (18). The *osgl-1* and *mtssb-1* RNAi feeding *E. coli* clones were purchased from the MRC Geneservice (Babraham Biocubator, Cambridge, UK). Synchronous L1 larvae were fed onto modified NGM plates seeded with *E. coli* HT115 expressing specific double stranded RNA as previously described (30). The plates were incubated routinely at 20°C. When worms reached adulthood they were transferred daily to fresh RNAi plates. The eggs were counted immediately after the removal of the parents; 24 h later, the oocytes, embryos and larvae were counted in order to evaluate embryonic lethality. The offspring phenotype was subsequently inspected for any striking phenotype. Subsequently, one L4 offspring has been selected and used for subsequent RNAi experiment using a similar phenotype analysis. This analysis has been pursued over three additional generations. The specificity and effectiveness of RNAi inactivation of *osgl-1* depletion in *eri-1* worms was checked by performing a semiquantitative RT-PCR analysis of *osgl-1* mRNA. Total RNA was isolated from *eri-1* animals fed on RNAi bacteria clones using Trizol reagent (Invitrogen). Seventy five ng of RNA from either RNAi control or *osgl-1(RNAi)* animals were treated with DNaseI, subsequently subjected to cDNA synthesis using SuperScript II reverse transcriptase (Invitrogen) and PCR amplified with TaqDNA polymerase (Invitrogen). The primers used were *osgl-1cDNAI* and *osgl-1cDNAr*. The amplification of a 426-bp fragment of the *ama-1* cDNA with primers *ama-1-f* and *ama-1-r* was used as internal control.

Pharmacological treatment

Paraquat (Sigma) was dissolved in water at 0.8 M and added to melted agar of NGM plates to a final concentration of 5 mM. The young adult RNAi animals were transferred onto Paraquat plates seeded with RNAi bacterial clones. The plates were incubated at 20°C and observed once a day for 10 days to count the number of dead worms. Worms were scored as dead when they no longer move in response to light touch.

Ethidium bromide (EB) (Sigma) was dissolved in water at 10 mg/ml and incorporated to melted NGM agar to the desired final concentrations. These plates were seeded with RNAi bacteria and *eri-1* L1 larvae were transferred. The plates were incubated at 20°C and tracked for 5 days by counting the number of worms that reach the gravid adult stage.

DAPI and Mitotracker staining

DNA analysis was performed by DAPI (4,6-diamidino-2-phenylindole; Sigma) staining. Yeast cells were harvested in exponential phase and fixed with 70% (v/v)

ethanol for 30 min and then washed two times with PBS. DAPI was added to a final concentration of 1 µg/ml and left in the dark for 5–10 min. Cells were washed and resuspended in a small volume and observed with a fluorescence microscope (see below). A culture of *E. coli* strain JO93 was grown in permissive conditions; the cells were harvested, washed and incubated overnight in permissive and non-permissive conditions. Cells were stained with DAPI as indicated above. Poor growth in the absence of arabinose required to concentrate the *E. coli* cells tenfold. Mitochondria were visualised using Mitotracker Red CMXRos (Molecular Probes), a red-fluorescent dye which stains mitochondria in live cells and for which uptake is membrane-potential dependant. Mitotracker Red was dissolved in DMSO.

Transgenic worms expressing *pie-1* promoter::*osgl-1*::*gfp::pie-1* 3'-UTR transgene were grown for 1 day at 20°C on NGM agar supplemented with 1 µg/ml Mitotracker Red CMXRos. Adult animals were transferred to a drop of M9 buffer 0.25 mM levamisole and dissected with a syringe needle to extrude the gonad and early embryos. Subsequently, gonads and eggs were transferred with a capillary pipette to agarose pads and mounted for microscopic observations.

Life-span assay

Caenorhabditis elegans life-span assays were performed at 20°C. *eri-1* synchronous L1 larvae were transferred to RNAi plates. Once the animals reached the adult stage they were transferred to fresh plates once a day to keep them separate from the offspring. The animals' viability was determined daily by assaying for movement in response to agitation of the plate or gentle prodding. Animals that did not respond to nose and tail prodding were scored as dead. Animals that crawled off the plate, exploded or bagged were censored.

Microscopy and image analysis

Epifluorescence images were collected using an inverted microscope (Leica DMIRE2) equipped with a digital camera. Acquisition software used was MetaMorph (Universal Imaging). Deconvolution analysis was performed with Metamorph Offline. The images were further processed and assembled with Adobe Photoshop 7.0.

RESULTS

Identification and phylogeny of Qri7 orthologs in Eukarya and Bacteria

We performed an up-to-date phylogenetic analysis of the whole Kael/YgjD/Qri7 family that strongly supports the emergence of eukaryotic Qri7 within bacterial YgjD/Gcp [posterior probability (PP) = 1.0, Supplementary Figure S1]. This analysis confirms our previous phylogenetic analysis (2). More precisely, the Qri7/Gcp eukaryotic sequences form a monophyletic group (PP = 1.0) and emerge as sister group of Alpha-Proteobacteria—albeit with a moderate statistical support (PP = 0.81), pointing to a mitochondrial origin. We performed an exhaustive

search of Qri7 homologs within complete or ongoing eukaryotic genomes (Supplementary Table S1). This showed that Qri7 proteins are ubiquitous in most eukaryotic supergroups, stressing the important role this protein would play in mitochondria. In fact, in agreement with a mitochondrial origin, Qri7 is absent from all genomes of amitochondriate eukaryotes (Microsporidia, Entamoeba and two excavate *Giardia lamblia* and *Trichomonas*). However, orthologs of this gene are also missing in some protists such as Kinetoplastids (a subgroup of Excavata) or in a number of Alveolata. The absence of Qri7 in available genomes of excavata is particularly appealing since representatives of this supergroup either lack mitochondria or have modified mitochondria (31). For example, Kinetoplastids have unique molecular features such as extensive RNA editing of mitochondrial genes that is templated by minicircle DNA (32). The Qri7 sequences found in few alveolata are highly divergent. Accordingly, the apparent absence of Qri7 in most Alveolata may be linked either to secondary losses or to a too high divergence (i.e. beyond detection) of the corresponding gene.

Escherichia coli *ygjD* mutant cells lose their nucleoid

We constructed an *E. coli* strain, JO93, carrying a conditional *ygjD* allele under the control of the arabinose operon promoter (see 'Materials and Methods' section). The JO93 mutant formed colonies of wild-type size on plates containing complete LB medium supplemented with 0.2% arabinose (expression of *ygjD*), whereas the strain failed to grow in the absence of arabinose (no expression of *ygjD*), indicating that YgjD is essential for growth in *E. coli*, in agreement with a previous report (13). Strain JO93 was grown overnight in permissive and non-permissive conditions and the resulting cells were observed under DAPI-epifluorescence microscopy (see 'Materials and Methods' section). In the absence of *ygjD* expression, *E. coli* cells displayed a reduced size and a high proportion lost their nucleoid (Figure 1).

A *S. cerevisiae* *qri7*-deletion mutant harbors mitochondria with abnormal morphology and no detectable DNA

According to the *Saccharomyces* Genome Database (<http://www.yeastgenome.org>), Qri7p is essential for respiration but dispensable for fermentation. In order to verify this phenotype, we compared the growth of the *S. cerevisiae* wild-type (Y00000) and *qri7*Δ (Y03801) mutant strains on solid complete media containing either glucose (YPD) or glycerol (YPG) as carbon sources. The wild-type strain was able to form colonies on both media, albeit more slowly on YPG, as expected. In contrast, the *qri7*Δ strain grew normally on YPD but failed to form colonies after five days on YPG, as previously reported (12) (Supplementary Figure S2). To determine if the absence of Qri7p has an effect on mitochondrial DNA, we investigated by microscopy analysis, DAPI stained samples of wild-type and *qri7*Δ cells (see 'Materials and Methods' section). Interestingly, whereas small fluorescent spots corresponding to mitochondrial DNA (mtDNA)

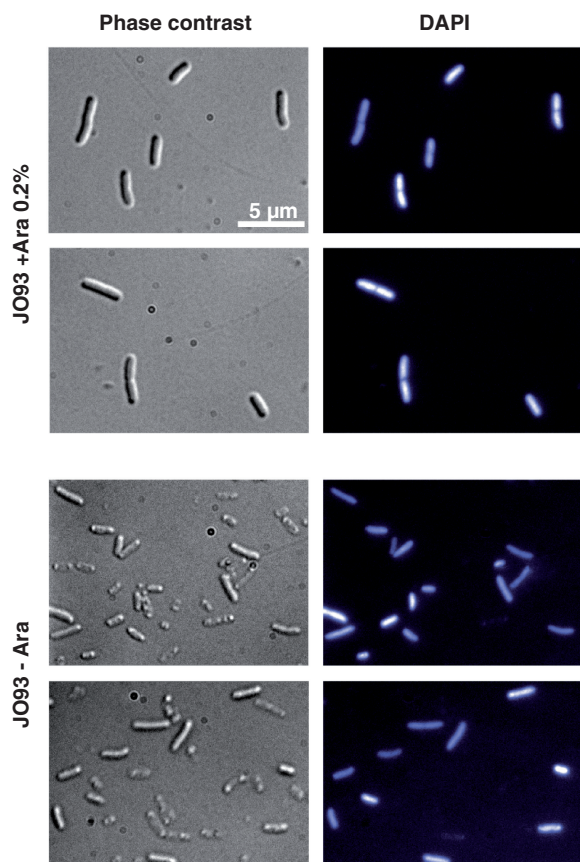


Figure 1. DAPI staining of *E. coli ygdD* cells in permissive and non-permissive conditions. *E. coli* strain JO93 was observed in permissive (top panels) and non-permissive conditions (bottom panels), under phase contrast (left panels) and after DAPI staining (right panels).

were clearly visible in wild-type cells beside the large spot corresponding to nuclear DNA, only the latter was visible in *qri7Δ* cells. This result indicated that *qri7Δ* mutants have lost mtDNA, while nuclear DNA was unaffected (Figure 2). The absence of detectable mtDNA in the yeast *qri7Δ* mutant observed by DAPI staining could be primarily associated with an alteration in mitochondrial morphology. To determine if it was the case, wild-type and *qri7Δ* mutant yeast cells were transformed with plasmid pXY142-mtGFP which expresses a mitochondria-targeted green fluorescent protein (33). The localization of mtGFP demonstrated that mitochondria were still present in the *qri7Δ* mutant. However, contrarily to wild-type cells where mitochondria form a tubular network, *qri7Δ* cells clearly showed highly fragmented mitochondria (Figure 3, left). These results have been confirmed by specific mitochondria staining of the same cells with the Mitotracker Red dye which is specifically oxidized to a fluorescent compound in mitochondria (Figure 3, right). In order to verify the absence of mitochondrial DNA in the *qri7Δ* mutant, a set of PCR reactions were performed on the total DNA extracted from wild-type and mutant cells (see ‘Materials and Methods’ section). The amplification of two individual mitochondrial DNA genes, encoding respectively the COX1 protein and the 21S rRNA yielded no detectable signal in the yeast mutant

(Figure 4). These data thus clearly indicate that loss of *QRI7* leads to the formation of mitochondria with abnormal morphology and no DNA.

Complementation of the *E. coli ygdD* conditional lethal mutant

A complementation test was designed to compare the function of the bacterial YgjD to that of its eukaryotic nuclear and mitochondrial counterparts, Kae1p and Qri7p. The conditional lethal *ygdD* allele was used for complementation tests with the *S. cerevisiae QRI7* gene (from which the 30 first codons, encoding the mitochondrial-targeting sequence were deleted) expressed from the pZE-JO vector (see ‘Materials and Methods’ section). The expression of *S. cerevisiae* mitochondrial Qri7p restored the viability of the YgjD mutant in non-permissive conditions (absence of arabinose) with a wild-type colony size indistinguishable from those obtained by complementation with a control plasmid carrying *ygdD*. In contrast, we obtained no complementation with the *S. cerevisiae KAE1* gene expressed in the same conditions (Supplementary Figure S3). This indicates that YgjD and Kae1 have either different functions or interact with different partners in Bacteria and Archaea/Eukarya, respectively. In agreement with this conclusion, Kae1 is known to interact in Eukarya and Archaea with the kinase Bud32(Prpk) which has no bacterial homolog (9,34).

The *C. elegans* Qri7 protein localizes to mitochondria

As expected, we identified two genes-encoding Qri7 homologs in the genome of *C. elegans*. The C01G10.10 protein corresponds to the *bona fide* Qri7p homolog (see Supplementary Figure S4 for an alignment with the yeast Qri7) whereas the Y71H2AM.1 protein is the nuclear Kae1/OSGEP ortholog. In agreement with these sequence data, we noticed that the amino-terminal region of C01G10.10 is predicted to be a mitochondrial targeting signal (iPSORT analysis, $P = 0.93$). For simplicity, we named the *C. elegans* C01G10.10 gene *osgl-1*. To confirm experimentally the mitochondrial localization of *osgl-1*, we constructed and expressed an *osgl-1::GFP* fusion construct in transgenic animals. The OSGL-1 fusion protein was under the control of the *pie-1* promoter and 3' UTR regulatory sequences, in order to enhance their expression in germ line cells of adult hermaphrodites and blastomeres of early *C. elegans* embryos (35). As shown in Figure 5, the OSGL-1::GFP was detected with a high intensity within the cytoplasm of both germ line cells of adult animals and blastomeres of early embryos and co-localized with the Mitotracker Red dye, indicating that the fusion protein had been indeed addressed to the mitochondria. We then examined, in transgenic animals, the *in vivo* expression pattern of OSGL-1::GFP when placed under the control of its own promoter (see ‘Materials and Methods’ section). The GFP signal was detected at a low level in most *C. elegans* cells. (Supplementary Figure S5). In agreement with its mitochondrial localization, the subcellular localization of the GFP signal in these cells was mostly cytoplasmic and somewhat similar to that of the *C. elegans* mitochondrial adenine nucleotide transporter ANT-1.1 (36).

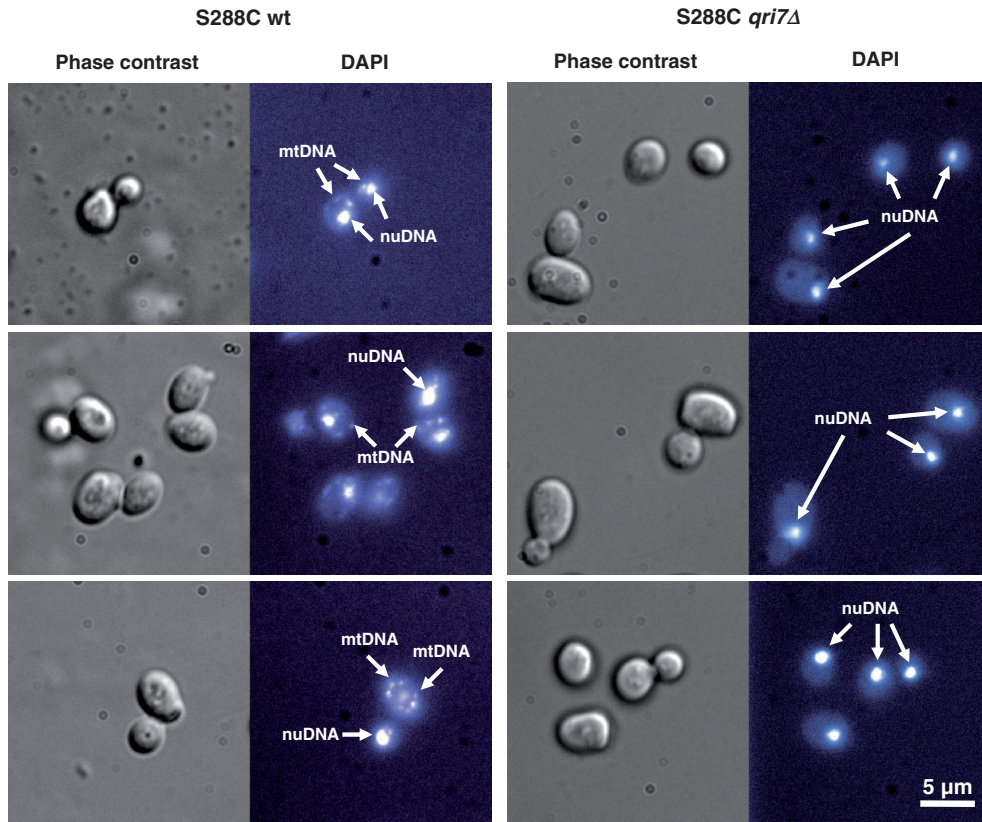


Figure 2. DAPI staining of wild-type and *qri7Δ* *S. cerevisiae* cells. Yeast strains S288C (wild-type) and S288C *qri7Δ* were observed under phase contrast (left panels) and after DAPI staining (right panels). mtDNA: mitochondrial DNA, nuDNA: nuclear DNA.

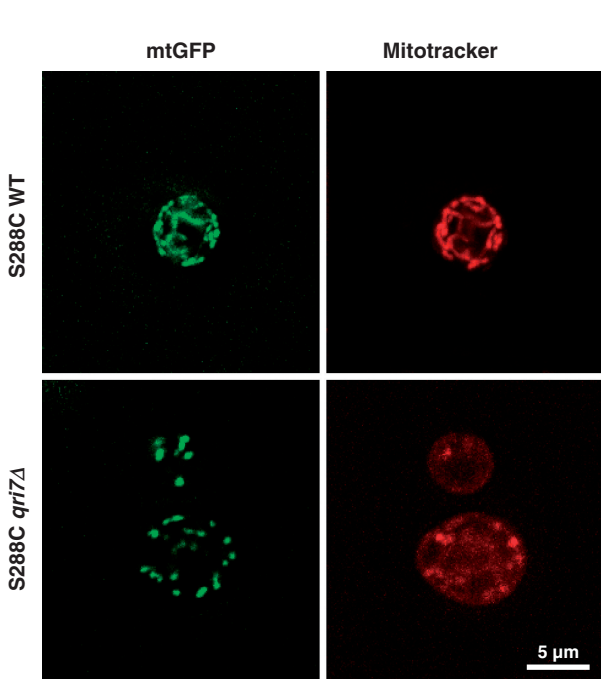


Figure 3. mtGFP and Mitotracker staining of wild-type and *qri7Δ* *S. cerevisiae* cells. Visualization of mtGFP in yeast strains S288C (wild-type) and S288C *qri7Δ* bearing plasmid pXY142-mtGFP (left). Mitotracker staining of the same strains (right).

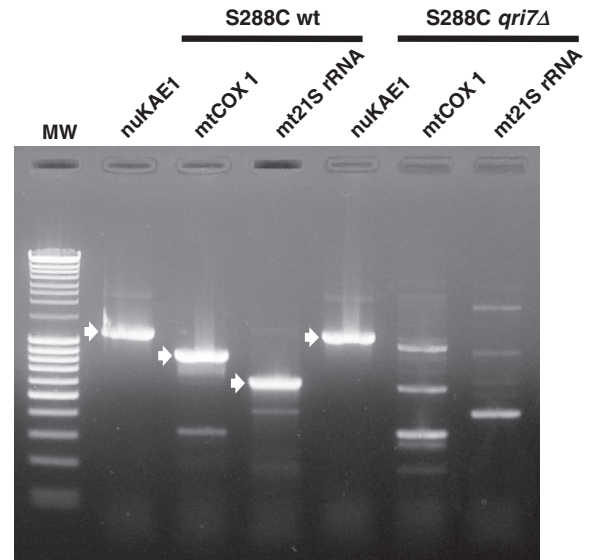


Figure 4. PCR amplification of total DNA extracted from in wild-type and *qri7Δ* *S. cerevisiae* cells. Oligonucleotide pair K1-pZE/K2-pZE, permitted to amplify a 1198-bp fragment corresponding to the chromosomal KAE1 gene, used as positive control. Oligonucleotide pairs (MT1/MT2 and MT3/MT4) amplified respectively a 909-bp fragment in the mitochondrial DNA gene COX1 and a 653-bp fragment in the mitochondrial DNA gene-encoding 21S rRNA. White arrows indicate the corresponding DNA fragments, when present, on the EB-stained agarose gel.

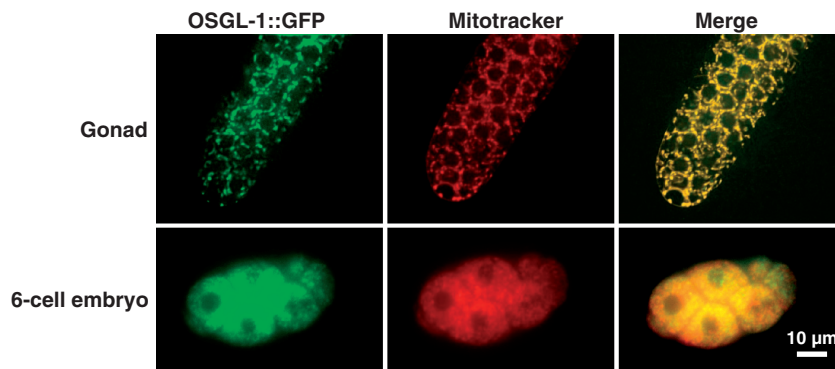


Figure 5. OSGL-1::GFP localizes to mitochondria. Transgenic N2 *C. elegans* expressing the OSGL-1 protein fused to GFP under the control of the *pie-1*-regulatory sequences were obtained by biolistic transformation. These animals were grown on NGM plate supplemented with Mitotracker Red. The OSGL-1 fusion protein colocalizes with mitochondria (red) in the embryos.

osgl-1 inactivation enhances longevity, resistance to oxidative stress and perturbs mitochondrial reticulum morphology

To further analyze the physiological role of *osgl-1* in *C. elegans*, we used the feeding RNAi technique (37) to disrupt the function of the protein. The *osgl-1* gene was inactivated in the *eri-1* genetic background, which is hypersensitive to RNAi (38) starting with L1 stage animals and over four consecutive generations, prior to any phenotype observations. We showed by RT-PCR that *osgl-1* mRNA was severely depleted in these conditions indicating that the *osgl-1* RNAi treatment was specific and efficient (Figure 6). Nevertheless, the *osgl-1*(RNAi) animals showed similar brood size and development to control animals over the successive generations (Supplementary Table S2).

Since mitochondria activity plays a key role in regulating *C. elegans* aging (39), we tested whether *osgl-1* is involved in the regulation of longevity. In parallel, we tested the phenotype of animals inactivated for the *mtssb-1* gene; MTSSB-1 is the single stranded mitochondrial DNA-binding protein which is essential for mitochondrial DNA replication (40). We observed that the RNAi inactivation of *osgl-1* lead to an increase of 10% ($P < 0.005$) in the *eri-1* mean longevity (Supplementary Figure S6). The involvement of *osgl-1* in *C. elegans* mitochondria physiology was further analyzed by exposing the *osgl-1*(RNAi) strain to the oxidative stressor paraquat. Often, reduced mitochondrial activity is correlated to a lower reactive oxygen species (ROS) production. Consistently, the *osgl-1*(RNAi) mutant was more resistant to oxidative stress induced by paraquat (Supplementary Figure S7A).

Recently, a novel role for p53 has been reported in mtDNA maintenance (41). In worms, p53/*cep-1* is required to mediate the germ cell line apoptosis and is involved in the oxidative stress response (42,43). We therefore tested the implication of *cep-1* in *osgl-1* paraquat resistance. We observed that *cep-1* inactivation reduced paraquat resistance of *osgl-1*(RNAi) animals (Supplementary Figure S7B). Therefore CEP-1 lowers the level of oxidative stress upon *osgl-1* inactivation.

To further analyze the involvement of *osgl-1* in the integrity of the mitochondrial network, we expressed in

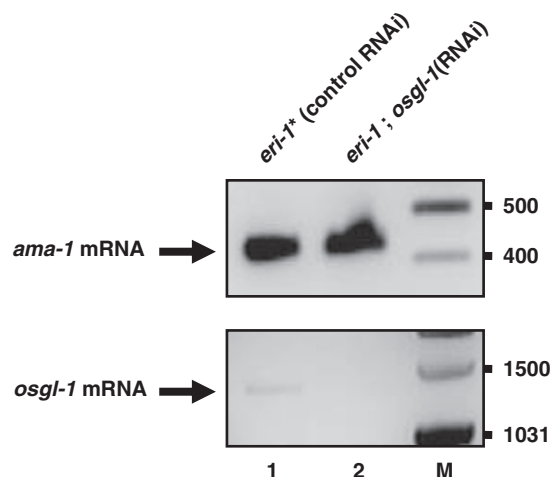


Figure 6. RNAi treatment efficiently reduced the *osgl-1* mRNA level. Simultaneous measurement of *ama-1* and *osgl-1* mRNA levels by Reverse transcriptase polymerase chain reaction (RT-PCR) analysis of total RNA isolated from *eri-1* animals grown on either the empty RNAi vector (lane 1) or *osgl-1* dsRNA-expressing bacteria (lane 2) during larval development and adulthood. Specific *osgl-1* mRNA is depleted in RNAi-treated animal (lane 2) as compared with RNA from the same gene in *eri-1* control animals (lane 1). The *ama-1* mRNA, a control gene encoding the catalytic core of the RNA polymerase II, was present at wild-type level in both conditions. This figure shows a negative of an EB-stained agarose gel. M: ladder DNA size marker.

C. elegans osgl-1(RNAi), a GFP protein targeted to the mitochondria in body wall muscle (BWM) cells. In control animals, BWM cells mitochondria appeared tubular and well organized along myofibrilla, whereas, in *osgl-1*(RNAi) mutants, the mitochondrial network was disorganized (Figure 7). This result indicates that *osgl-1* inactivation affects the mitochondrial reticulum shape and strongly resembles the effect of Qri7 loss on the morphology of yeast mitochondria.

Ethidium Bromide sensitivity of *osgl-1*(RNAi) mutants

To analyze *osgl-1* involvement in mitochondrial genome maintenance, we tested the sensitivity of *osgl-1*(RNAi) mutants to EB. EB is known to preferentially inhibit

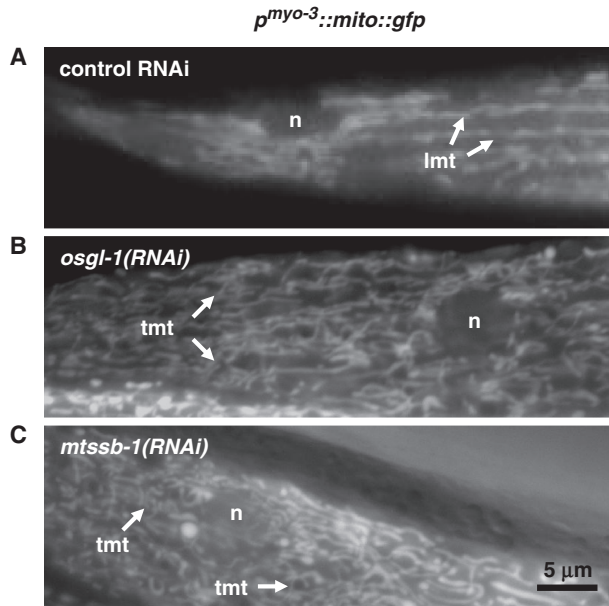


Figure 7. *osgl-1(RNAi)* mutants show alteration of the mitochondria reticulum in BWM cells. The *osgl-1* and *mtssb-1* genes were inactivated by RNAi in the wild-type strain expressing *pmyo3::mito::GFP*. In control RNAi animals, BWM cells have tubular mitochondria that run parallel to the cell axis (A), whereas the mitochondria reticulum of both *osgl-1(RNAi)* (B) and *mtssb-1(RNAi)* mutants (C) is disorganized. The tubular section is thinner, and tubules are not well aligned along the BWM cell myofilament with connecting strands between tubules (black arrows). The density of tubules forming the reticulum is higher in both mutants (B, C) than in the control animal (A). n: nucleus, lmt: longitudinal mitochondrial tubule, tmt: transversal mitochondrial tubule.

mitochondrial DNA replication and transcription, which causes mitochondrial DNA depletion. It has been reported that *S. cerevisiae* cells lacking mitochondrial single-stranded DNA-binding protein ABF2 are hypersensitive to EB (44). The nematode *C. elegans* survives on media supplemented with EB but displays increased generation time and/or a block at the L3 stage of development (40,45). The *eri-1;osgl-1(RNAi)* mutants were compared with *eri-1* animals in their capacity to grow and develop to the adult stage in the presence of increasing concentrations of EB. In parallel, we tested the sensitivity of the *eri-1;mtssb-1(RNAi)* mutant (Figure 8). We observed that animals with *osgl-1* RNAi inactivation are more sensitive to EB. The *eri-1* control animals have an EC_{50} for EB of circa 40 $\mu\text{g/ml}$, whereas the *eri-1;osgl-1(RNAi)* mutant animals have an EC_{50} of circa 32 $\mu\text{g/ml}$. This is a consistent slight difference which is further illustrated, as shown in Figure 8, at the concentration of 40 $\mu\text{g/ml}$, 50% of the *eri-1* control animals reached the adult stage whereas only 20% of the double mutant *eri-1;osgl-1(RNAi)* still developed to adulthood. The increased sensitivity to EB was also observed in the *eri-1;mtssb-1(RNAi)* mutant which is in agreement with what was observed in the corresponding *S. cerevisiae* *abf2* mutant (44). Although the effect of EB was less drastic on the *osgl-1(RNAi)* mutant than on the *mtssb-1(RNAi)* mutant, the increased sensitivity of *osgl-1(RNAi)* mutant to EB suggest that OSGL-1 participates

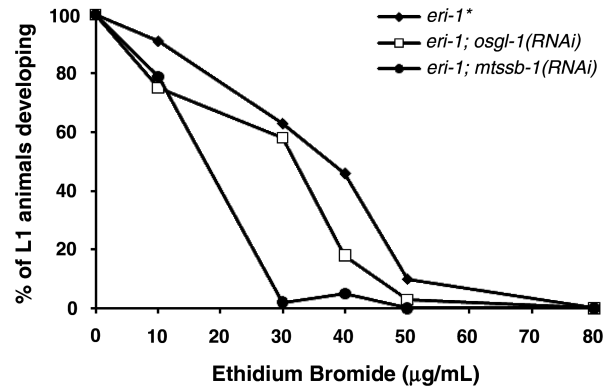


Figure 8. *osgl-1(RNAi)* mutants are hypersensitive to the EB induced mitochondrial DNA depletion. The ability of the *eri-1*, *eri-1;osgl-1(RNAi)* and *eri-1;mtssb-1(RNAi)* L1 larvae to grow and develop to adulthood on increasing concentration of EB was analyzed. The *eri-1* L1 animals were grown on bacteria expressing dsRNA of *osgl-1* or *mtssb-1* genes or containing the empty RNAi vector only (asterisk). The percentage of L1 animals developing is indicated. The experiment was performed at 20°C. Each point corresponds to the analysis of $n > 40$ animals.

somehow in the mitochondrial genome maintenance as in *S. cerevisiae*.

DISCUSSION

We have presented here evidences that *qri7/osgl-1* is essential for mitochondrial genome maintenance in both *C. elegans* and *S. cerevisiae*. This role is probably conserved in all eukaryotes with mitochondria, since Qri7 are very well conserved proteins. The basic biological function of Qri7 is probably also conserved in Bacteria, since Qri7 from *S. cerevisiae* fully complements an *E. coli* mutant lacking the essential protein YgjD (the bacterial Qri7 homolog). Furthermore, we observed that an *E. coli* *ygd* mutant strain displays frequent nucleoid loss. In a recent report, *E. coli* proteins YeaZ and YjeE were proposed as essential partners for YgjD function (14). The YgjD/Qri7 complementation results we observed in *E. coli* thus indicate that the yeast Qri7 protein should be able to interact correctly with YeaZ and YjeE in this bacterium, despite the fact that YeaZ and YjeE have no detectable homologs in *S. cerevisiae* and *C. elegans* (BLASTp E -values ≥ 0.31).

The archaeal protein Kae1 (homologous to Qri7 and YgjD) binds DNA and exhibits an atypical AP endonuclease activity *in vitro* (9,34), whereas the nuclear eukaryotic protein Kae1 is member of the KEOPS/EKC complex which is associated to chromatin and involved in telomere maintenance (8,10).

These data, together with the results presented here, indicate that Kae1/OSGEP/Qri7/YgjD form a new family of proteins probably essential for genome stability in all organisms from the three domains of life. The precise *in vivo* biochemical role of these proteins remains to be determined. The *in vitro* data obtained with the archaeal protein suggest that they could both recognize DNA damage and play an architectural role in chromatin organization. It should be stressed that very few universal

proteins are known to be involved in DNA metabolism (46). One of them is the universal recombinase (called RecA in Bacteria, Rad51 and paralogs in Eukarya, and RadA, RadB in Archaea) that plays a critical role in homologous DNA recombination and DNA repair. We predict that the importance of essential proteins of the Kae1/OSGEP/Qri7/YgjD family would rival those of RecA and its homologs in the maintenance of genome integrity in all living cells. To avoid further confusion in the nomenclature, we propose to rename UGMP (Universal Genome Maintenance Proteins) all proteins of the Kae1/Qri7/OSGEP/YgjD family.

Interestingly, the gene encoding the human Qri7 ortholog (OSGL) is localized in a region of the chromosome 2q32, which is involved in several human diseases (47). Considering the high number of pathologies associated to mitochondrial defects and the importance of Qri7/OSGEP in mitochondrial physiology, it is reasonable to speculate that deficiency in the normal function of this protein could lead to important pathologies in human. Indeed, the *C. elegans osgep-1* mutants are viable, although sensitive to EB, suggesting that multicellular individuals with mutated Qri7 versions (or even lacking Qri7) could be viable carriers of potentially harmful defects.

SUPPLEMENTARY DATA

Supplementary Data are available at NAR Online.

ACKNOWLEDGEMENTS

We thank Dr A. Fire for providing pPD plasmids and G. Seydoux for the gateway cloning destination vector. The nematode strains used in this work were provided by the *Caenorhabditis* Genetics Center, which is funded by the National Institutes of Health, National Center for Research Resources.

FUNDING

Centre National de la Recherche Scientifique (CNRS); Agence Nationale de la Recherche; Association pour la Recherche sur le Cancer (ARC); Ministère de la Recherche fellowship (to N.B.); Action Thématique et Incitative sur Programme (ATIP) of the Centre National de la Recherche Scientifique (to C.B.-A.). Funding for open access charge: ANR.

Conflict of interest statement. None declared.

REFERENCES

- Galperin, M.Y. and Koonin, E.V. (2004) 'Conserved hypothetical' proteins: prioritization of targets for experimental study. *Nucleic Acids Res.*, **32**, 5452–5463.
- Hecker, A., Leulliot, N., Gabelle, D., Graille, M., Justome, A., Dorlet, P., Brochier, C., Quevillon-Cheruel, S., Le Cam, E., van Tilbeurgh, H. *et al.* (2007) An archaeal orthologue of the universal protein Kae1 is an iron metalloprotein which exhibits atypical DNA-binding properties and apurinic-endonuclease activity in vitro. *Nucleic Acids Res.*, **35**, 6042–6051.
- Galperin, M.Y. (2008) Social bacteria and asocial eukaryotes. *Environ. Microbiol.*, **10**, 281–288.
- Abdullah, K.M., Lo, R.Y. and Mellors, A. (1991) Cloning, nucleotide sequence, and expression of the *Pasteurella haemolytica* A1 glycoprotease gene. *J. Bacteriol.*, **173**, 5597–5603.
- Abdullah, K.M., Udoh, E.A., Shewen, P.E. and Mellors, A. (1992) A neutral glycoprotease of *Pasteurella haemolytica* A1 specifically cleaves O-sialoglycoproteins. *Infect. Immun.*, **60**, 56–62.
- Nichols, C.E., Johnson, C., Lockyer, M., Charles, I.G., Lamb, H.K., Hawkins, A.R. and Stammers, D.K. (2006) Structural characterization of *Salmonella typhimurium* YeaZ, an M22 O-sialoglycoprotein endopeptidase homolog. *Proteins*, **64**, 111–123.
- Roberts, R.J. (2004) Identifying protein function – a call for community action. *PLoS Biol.*, **2**, E42.
- Downey, M., Houlsworth, R., Maringe, L., Rollic, A., Brehme, M., Galicia, S., Guillard, S., Partington, M., Zubko, M.K., Krogan, N.J. *et al.* (2006) A genome-wide screen identifies the evolutionarily conserved KEOPS complex as a telomere regulator. *Cell*, **124**, 1155–1168.
- Hecker, A., Lopreiato, R., Graille, M., Collinet, B., Forterre, P., Libri, D. and van Tilbeurgh, H. (2008) Structure of the archaeal Kae1/Bud32 fusion protein MJ1130: a model for the eukaryotic EKC/KEOPS subcomplex. *EMBO J.*, **27**, 2340–2351.
- Kisseleva-Romanova, E., Lopreiato, R., Baudin-Baillieu, A., Rousselle, J.C., Ilan, L., Hofmann, K., Namane, A., Mann, C. and Libri, D. (2006) Yeast homolog of a cancer-testis antigen defines a new transcription complex. *EMBO J.*, **25**, 3576–3585.
- Huh, W.K., Falvo, J.V., Gerke, L.C., Carroll, A.S., Howson, R.W., Weissman, J.S. and O'Shea, E.K. (2003) Global analysis of protein localization in budding yeast. *Nature*, **425**, 686–691.
- Steinmetz, L.M., Scharfe, C., Deutschbauer, A.M., Mokranjac, D., Herman, Z.S., Jones, T., Chu, A.M., Giaever, G., Prokisch, H., Oefner, P.J. *et al.* (2002) Systematic screen for human disease genes in yeast. *Nat. Genet.*, **31**, 400–404.
- Arigoni, F., Talabot, F., Peitsch, M., Edgerton, M.D., Meldrum, E., Allet, E., Fish, R., Jamotte, T., Curchod, M.L. and Loferer, H. (1998) A genome-based approach for the identification of essential bacterial genes. *Nat. Biotechnol.*, **16**, 851–856.
- Handford, J.L., Ize, B., Buchanan, G., Butland, G.P., Greenblatt, J., Emili, A. and Palmer, T. (2009) Conserved network of proteins essential for bacterial viability. *J. Bacteriol.* doi:10.1128/JB.00136-09.
- Datsenko, K.A. and Wanner, B.L. (2000) One-step inactivation of chromosomal genes in *Escherichia coli* K-12 using PCR products. *Proc. Natl Acad. Sci. USA*, **97**, 6640–6645.
- Silhavy, T.J., Berman, M.L. and Enquist, L.W. (1984) *Experiments with Gene Fusions*. Cold Spring Harbor Laboratory, Cold Spring Harbor, NY.
- Sherman, F. (1991) Getting started with yeast. *Methods Enzymol.*, **194**, 3–21.
- Timmons, L. and Fire, A. (1998) Specific interference by ingested dsRNA. *Nature*, **395**, 854.
- Guzman, L.M., Belin, D., Carson, M.J. and Beckwith, J. (1995) Tight regulation, modulation, and high-level expression by vectors containing the arabinose PBAD promoter. *J. Bacteriol.*, **177**, 4121–4130.
- Lutz, R. and Bujard, H. (1997) Independent and tight regulation of transcriptional units in *Escherichia coli* via the LacR/O, the TetR/O and AraC/I1-I2 regulatory elements. *Nucleic Acids Res.*, **25**, 1203–1210.
- Praitis, V., Casey, E., Collar, D. and Austin, J. (2001) Creation of low-copy integrated transgenic lines in *Caenorhabditis elegans*. *Genetics*, **157**, 1217–1226.
- Walhout, A.J., Temple, G.F., Brasch, M.A., Hartley, J.L., Lorson, M.A., van den Heuvel, S. and Vidal, M. (2000) GATEWAY recombinational cloning: application to the cloning of large numbers of open reading frames or ORFeomes. *Methods Enzymol.*, **328**, 575–592.
- D'Agostino, I., Merritt, C., Chen, P.L., Seydoux, G. and Subramaniam, K. (2006) Translational repression restricts expression of the *C. elegans* Nanos homolog NOS-2 to the embryonic germline. *Dev. Biol.*, **292**, 244–252.
- Altschul, S.F., Madden, T.L., Schaffer, A.A., Zhang, J., Zhang, Z., Miller, W. and Lipman, D.J. (1997) Gapped BLAST and

- PSI-BLAST: a new generation of protein database search programs. *Nucleic Acids Res.*, **25**, 3389–3402.
25. Edgar, R.C. (2004) MUSCLE: multiple sequence alignment with high accuracy and high throughput. *Nucleic Acids Res.*, **32**, 1792–1797.
 26. Philippe, H. (1993) MUST, a computer package of management utilities for sequences and trees. *Nucleic Acids Res.*, **21**, 5264–5272.
 27. Ronquist, F. and Huelsenbeck, J.P. (2003) MrBayes 3: Bayesian phylogenetic inference under mixed models. *Bioinformatics*, **19**, 1572–1574.
 28. Oberto, J. (2008) BAGET: a web server for the effortless retrieval of prokaryotic gene context and sequence. *Bioinformatics*, **24**, 424–425.
 29. Hoffman, C.S. and Winston, F. (1987) A ten-minute DNA preparation from yeast efficiently releases autonomous plasmids for transformation of *Escherichia coli*. *Gene*, **57**, 267–272.
 30. Kamath, R.S., Fraser, A.G., Dong, Y., Poulin, G., Durbin, R., Gotta, M., Kanapin, A., Le Bot, N., Moreno, S., Sohrmann, M. *et al.* (2003) Systematic functional analysis of the *Caenorhabditis elegans* genome using RNAi. *Nature*, **421**, 231–237.
 31. Simpson, A.G. and Roger, A.J. (2004) The real ‘kingdoms’ of eukaryotes. *Curr. Biol.*, **14**, R693–R696.
 32. Simpson, A.G., Lukes, J. and Roger, A.J. (2002) The evolutionary history of kinetoplastids and their kinetoplasts. *Mol. Biol. Evol.*, **19**, 2071–2083.
 33. Westermann, B. and Neupert, W. (2000) Mitochondria-targeted green fluorescent proteins: convenient tools for the study of organelle biogenesis in *Saccharomyces cerevisiae*. *Yeast*, **16**, 1421–1427.
 34. Hecker, A., Graille, M., Madec, E., Gabelle, D., Le Cam, E., van Tilbergh, H. and Forterre, P. (2009) The universal Kae1 protein and the associated Bud32 kinase (PRPK), a mysterious protein couple probably essential for genome maintenance in Archaea and Eukarya. *Biochem. Soc. Trans.*, **37**, 29–35.
 35. Strome, S., Powers, J., Dunn, M., Reese, K., Malone, C.J., White, J., Seydoux, G. and Saxton, W. (2001) Spindle dynamics and the role of gamma-tubulin in early *Caenorhabditis elegans* embryos. *Mol. Biol. Cell*, **12**, 1751–1764.
 36. Farina, F., Alberti, A., Breuil, N., Bolotin-Fukuhara, M., Pinto, M. and Culetto, E. (2008) Differential expression pattern of the four mitochondrial adenine nucleotide transporter ant genes and their roles during the development of *Caenorhabditis elegans*. *Dev. Dyn.*, **237**, 1668–1681.
 37. Kamath, R.S. and Ahringer, J. (2003) Genome-wide RNAi screening in *Caenorhabditis elegans*. *Methods*, **30**, 313–321.
 38. Kennedy, S., Wang, D. and Ruvkun, G. (2004) A conserved siRNA-degrading RNase negatively regulates RNA interference in *C. elegans*. *Nature*, **427**, 645–649.
 39. Dillin, A., Hsu, A.L., Arantes-Oliveira, N., Lehrer-Graiwer, J., Hsin, H., Fraser, A.G., Kamath, R.S., Ahringer, J. and Kenyon, C. (2002) Rates of behavior and aging specified by mitochondrial function during development. *Science*, **298**, 2398–2401.
 40. Sugimoto, T., Mori, C., Takanami, T., Sasagawa, Y., Saito, R., Ichiishi, E. and Higashitani, A. (2008) *Caenorhabditis elegans* par2.1/msbb-1 is essential for mitochondrial DNA replication and its defect causes comprehensive transcriptional alterations including a hypoxia response. *Exp. Cell Res.*, **314**, 103–114.
 41. Achanta, G., Sasaki, R., Feng, L., Carew, J.S., Lu, W., Pelicano, H., Keating, M.J. and Huang, P. (2005) Novel role of p53 in maintaining mitochondrial genetic stability through interaction with DNA Pol gamma. *EMBO J.*, **24**, 3482–3492.
 42. Masse, I., Molin, L., Mouchiroud, L., Vanhems, P., Palladino, F., Billaud, M. and Solari, F. (2008) A novel role for the SMG-1 kinase in lifespan and oxidative stress resistance in *Caenorhabditis elegans*. *PLoS ONE*, **3**, e3354.
 43. Schumacher, B., Hofmann, K., Boulton, S. and Gartner, A. (2001) The *C. elegans* homolog of the p53 tumor suppressor is required for DNA damage-induced apoptosis. *Curr. Biol.*, **11**, 1722–1727.
 44. Chen, X.J., Wang, X., Kaufman, B.A. and Butow, R.A. (2005) Aconitase couples metabolic regulation to mitochondrial DNA maintenance. *Science*, **307**, 714–717.
 45. Tsang, W.Y. and Lemire, B.D. (2002) Mitochondrial genome content is regulated during nematode development. *Biochem. Biophys. Res. Commun.*, **291**, 8–16.
 46. Leipe, D.D., Aravind, L. and Koonin, E.V. (1999) Did DNA replication evolve twice independently? *Nucleic Acids Res.*, **27**, 3389–3401.
 47. Occhi, G., Olivieri, M., Rampazzo, A. and Danieli, G.A. (2004) Characterization of a novel human gene containing ANK repeats and ARM domains. *Biochem. Biophys. Res. Commun.*, **318**, 38–45.